Korean J. Chem. Eng., 33(7), 2027-2033 (2016)
DOI: 10.1007/s11814-016-0054-1

pISSN: 0256-1115
eISSN: 1975-7220

Ni^{2+} reduction under solar irradiation over $CuFe_2O_4/TiO_2$ catalysts

Maamar Fedailaine, Sabrina Berkani, and Mohamed Trari†

Laboratory of Storage and Valorization Renewable Energies (USTHB), BP 32 El-Alia 16111 Algiers, Algeria
(*Received 31 December 2014 • accepted 22 February 2016*)

Abstract−The photo-electrochemical characterization of the hetero-system $CuFe_2O_4/TiO_2$ was undertaken for the Ni^{2+} reduction under solar light. The spinel $CuFe_2O_4$ was prepared by nitrate route at 940 °C and the optical gap (1.66 eV) was well matched to the sun spectrum. The flat band potential (−0.21 V_{SCE}) is more cathodic than the potential of Ni^{2+}/Ni couple (−0.6 V_{SCE}), thus leading to a feasible nickel photoreduction. TiO_2 with a gap of 3.2 eV is used to mediate the electrons transfer. The reaction is achieved in batch configuration and is optimized with respect to Ni^{2+} concentration (30 ppm); a reduction percentage of 72% is obtained under sunlight, the Ni^{2+} reduction is strongly enhanced and follows a first order kinetic with a rate constant of 4.6×10^{-2} min^{-1} according to the Langmuir-Hinshelwood model.

Keywords: Photocatalysis, Spinel $CuFe_2O_4$, Nickel, Sunlight

INTRODUCTION

The removal of inorganic pollutants like toxic metals from wastewaters is currently one of the most important topics in the environmental protection [1]. Aquatic pollution mainly comes from industrial landfills like batteries, plating and paint. Unlike organic molecules, heavy metals are non-biodegradable and resistant to both chemical and biological treatment [2]. Humans can be exposed to nickel-based compounds through breathing, drinking water, eating food and skin contact with contaminated soil and water [3]. Absorption of excessive amounts of nickel increases the risk of developing cancer of lung, larynx and prostate [4,5]. So, the threshold concentration of nickel is drastically limited at 0.5 ppm by the World Health Organization [5]. The conventional methods usually employed for the nickel removal, such as adsorption, electro reduction and reverse osmosis, are relatively high cost and become often inefficient at low concentrations. In this respect, the heterogeneous photocatalysis emerged as a clean alternative for the reduction of metals to less harmful forms and elemental states [6]. Solar energy represents an inexhaustible energetic resource with a high solar constant at the sea level [7]. Semiconductor oxides like SnO_2 [8], TiO_2 [8,9] and ZnO [10] are chemically stable against corrosion but possess a large gap (E_g>3 eV) and are technically unattractive for the exploitation of the solar radiation, which entails only ~5% of UV light. In this regard, other families such as the delafossites [10,11] and spinels have been tested in photocatalysis [12,13], as no systematic works have been undertaken in the metals removal over these materials [14]. The choice of the spinel $CuFe_2O_4$ as photocatalyst is motivated by its environmental friendly characteristics: light absorption over the whole solar spectrum [15], chemical stability in a wide pH range, and low-cost. The oxide was prepared by nitrate route in order to have a large active surface and a narrow crystallites size distribution. The aim of the present work is the elimination of nickel from the aquatic medium using the hetero-junction $CuFe_2O_4/TiO_2$ as catalyst under solar irradiation. The electron transfer in heterogeneous photocatalysis occurs iso-energetically and TiO_2 is used as electron bridge between the spinel, acting as sensitizer, and Ni^{2+}.

EXPERIMENTAL

CuO and $Fe(NO_3)_2$, $9H_2O$, both of analytical purity, with a molar ratio (Fe/Cu=2) were dissolved in HNO_3 (9 N); the solution was evaporated and denitrified on a hot plate until there were no NO_x fumes. At this level, 20 mg was removed and the thermal decomposition (TG) of the amorphous powder was examined in a Setaram thermo analyzer (AG0084 Labosystem). The powder (~10 g) was ground in an agate mortar and heated at 940 °C. The phase was identified by X-ray diffraction over the 2θ range (10-80°) using Cu K_α radiation (λ=0.154178 nm). The morphology of the oxides was examined by scanning electron microscopy (SEM, Nicoplet 235) working at 20 kV. The specific surface area of the powder was measured before and after the photocatalytic test by the BET method using nitrogen gas as adsorbate at liquid nitrogen temperature on ASAP 2010 Micromeritics apparatus.

The Ni^{2+} stock solution (2,000 ppm) was prepared by dissolving an accurate quantity of $NiSO_4$, $6H_2O$ (Merck, 99%) in distilled water (~0.8 MΩ cm); six concentration solutions (10, 30, 50, 75, 100 and 125 ppm) were prepared by dilution of the 2,000 ppm solution with distilled water. The photocatalytic reactions were carried out in batch mode using a double walled Pyrex reactor with 0.5 cm of water as cut off heating effects; the temperature fluctuates between 20 and 24 °C (Fig. 1). The powder, with a mass ratio equal to unity, i.e., ($CuFe_2O_4/TiO_2$=100 mg/100 mg), was uniformly dispersed by magnetic stirring (250 rpm) and exposed to sunlight by clear weather. In all experiments, the catalyst dose (200 mg catalyst/200 mL solu-

†To whom correspondence should be addressed.
E-mail: solarchemistry@gmail.com

Fig. 1. The experimental set up for the solar photocatalysis.

tion) was maintained constant. The aliquots were withdrawn at regular time intervals and centrifuged (3,000 rpm, 5 mn) to separate the solid particles from the supernatant. The residual Ni^{2+} concentration was analyzed with a UV-Visible spectrophotometer (Shimadzu 1800). The Ni^{2+} solution was mixed with dimethylglyoxime in presence of $K_2S_2O_8$ in ammonia solution. According to the Beer Lambert law, the red-brown complex $Ni(HDm)_2$ presents a maximum absorption at 465 nm with a molar absorption coefficient of 16000 and a sensitivity of 2 ppm. At at this level, $S_2O_3^{2-}$ was tested as reducing agent, but in vain, as the photoactivity decreased to 25%.

Hydrogen evolution method was used to confirm the nickel deposition. Owing to its redox potential (−0.25 V_{SCE}), nickel was re-dissolved in acid medium according to the reaction: $Ni^0+2\,H^+ \rightarrow Ni^{2+}+H_2$; the powder was attacked by HCl solution (4 N) and the liberated hydrogen was qualitatively identified by TCD chromatograph (IGC 121 ML) containing two 4 m carbosieve B columns (1/8 in., 100-200 meshes) with a catharometer detector and argon as carrier gas (sensitivity to ±2 μL).

Over illumination, the Ni^{2+} reduction was slowed down because of the competitive water reduction ($H_2O+2\,e^- \rightarrow H_2+OH^-$). The quantity of hydrogen was reliably determined volumetrically by water displacement due to the pressure developed inside the closed reactor.

EVALUATION OF SOLAR RADIATION

The black spinel $CuFe_2O_4$ activated by visible light acts as electron pump and generates free radicals via TiO_2 (Degussa-P25). All experiments are carried out under sunlight outside our Laboratory (latitude 36.78° North, longitude 3.05° West). The energy collected by the reactor (per unit area) is expressed as [16]:

$$Q_n = Q_{n-1} + \Delta t_n I_n A_r V_T^{-1} \quad (1)$$

$$\Delta t_n = t_n - t_{n-1} \quad (2)$$

where t_n is the experiment time for which the aliquot is withdrawn, I_n the average global irradiation during the period Δt_n, A_r the irradiated surface, V_T the total volume and Q_n the accumulated energy (per unit volume, kJ L^{-1}) reaching the reactor. When Q_n is used instead time, the reaction rate is expressed in terms of pollutant mass (mg) converted per kJ of global irradiation reaching the collector surface. Eq. (1) allows a comparison of experiments with different values of I_n, A_r and V_T.

RESULTS AND DISCUSSION

The spinel $CuFe_2O_4$ was prepared by nitrate route and the different stages are highlighted by thermal analysis. The main weight losses in the TG plot (Fig. 2(a)) start at ~70 °C and end at ~400 °C and are attributed to water departure (170 °C) [17] and nitrates decomposition of iron (~165 °C) and copper (~250 °C), respectively, as confirmed by the peaks in the DTG plot. The plateau region (500-900 °C) indicates the spinel formation with the presence of CuO (tenorite) and Fe_2O_3 (hematite) as impurities. By contrast, the XRD pattern of the sample heated at 940 °C (Fig. 2(b)) is characteristic of $CuFe_2O_4$ single phase with noticeably narrow peaks and good crystallization. All peaks are indexed in a tetragonal symmetry in agreement with the JCPDS card N° 34-0425. The morphology of the powder strongly depends on the synthesis con-

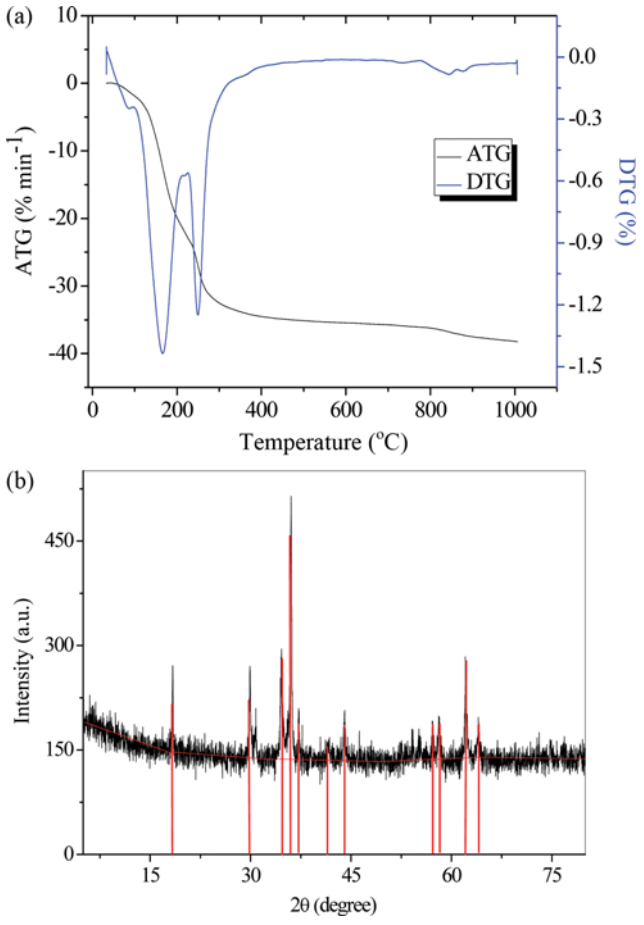

Fig. 2. (a) TGA plot of iron and copper nitrates mixture, heating rate 5 °C mn^{-1}. (b) The XRD pattern of $CuFe_2O_4$.

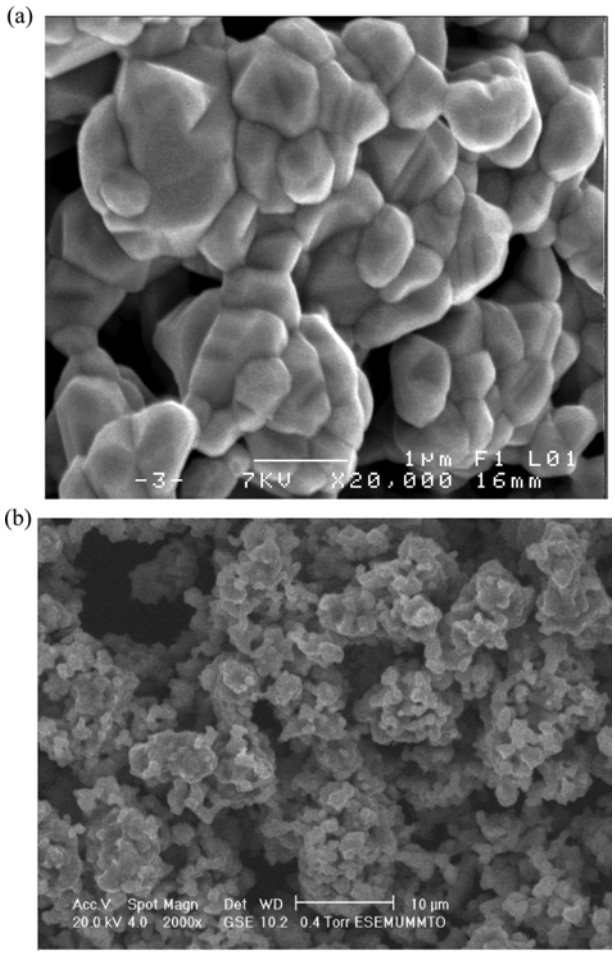

Fig. 3. The SEM images of $CuFe_2O_4$ powder (a) TiO_2 powder (b).

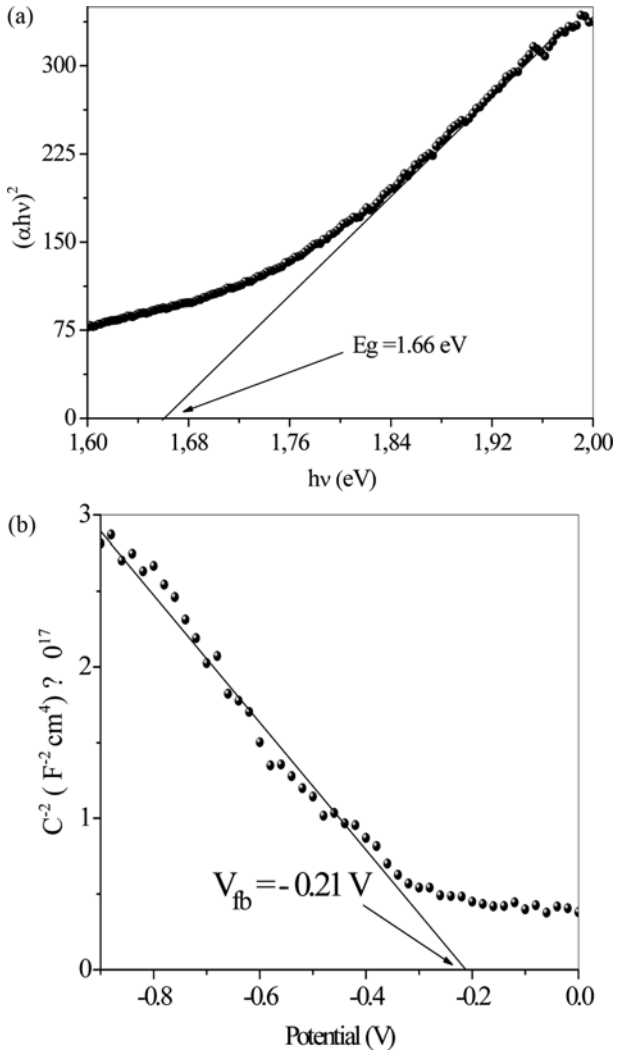

Fig. 4. (a) The direct optical transition of the spinel $CuFe_2O_4$. (b) The Mott-Schottky plot of $CuFe_2O_4$ in the working solution (Ni^{2+} 30 ppm, pH~7).

ditions. The SEM image of $CuFe_2O_4$ powder (Fig. 3) shows a compact nature with a micro structural morphology and crystallites agglomerates with an average size of 0.5 μm (Fig. 3(a)). By contrast, TiO_2 is porous with more or less circular forms of variable diameters (Fig. 3(b)).

The optical gap (E_g) is an important parameter and a value of ~1.5 eV is desirable in the solar energy conversion. The fundamental optical absorption is used to determine the nature of the transition and its value:

$$(\alpha h\nu)^{1/n}=A\,(h\nu-E_g) \quad (3)$$

A is a constant. The extrapolation of the linear part $(\alpha h\nu)^{1/n}$ to the energy axis indicates a direct gap (1.66 eV) attributed to *d-d* transition (Fig. 4(a)), which can be reasonably taken as the optical gap, due to the black color. It is of interest to discuss briefly the origin of such transition; with five *3d* electrons in the octahedrally coordinated Fe^{3+} site, the lower filled t_{2g} provides the valence band while the conduction band consists of empty e_g orbital.

A knowledge of the flat band potential V_{fb} is crucial in photocatalysis since it gives the position of the conduction band (−0.21 V); such value is provided from the intercept of the linear plot of the Mott-Schottky characteristic with the potential-axis at $C^{-2}=0$ (Fig. 4(b)):

$$C^{-2}=(2/e\varepsilon\varepsilon_o N_D)\,\{V-V_{fb}\} \quad (4)$$

where all symbols have their usual significations; the negative slope lends a further support of *p* type conduction of the spinel $CuFe_2O_4$. The energy diagram (Fig. 5), drawn from the photo-electrochemical characterization, is a preamble of photocatalysis; it clearly shows the feasibility of Ni^{2+} reduction on the hetero-system under illumination. Indeed, the potential of the conduction band is negative enough to reduce Ni^{2+} into elemental state. However, the large difference between the conduction band of the spinel (CB-$CuFe_2O_4$= −1.9 V) and the Ni^{2+} level (~ −0.6 V for 30 ppm) makes the rate of electrons transfer weak. So, a wide band gap semiconductor is needed and the electrons are transferred to Ni^{2+} ions via the conduction band of TiO_2 (~ −0.70 V), which works as electron bridge according to the following scheme:

$$p\text{-}CuFe_2O_4+h\nu\rightarrow CB\text{-}CuFe_2O_4\,(e^-)+VB\text{-}CuFe_2O_4\,(h^+) \quad (5)$$

$$CB\text{-}CuFe_2O_4\,(e^-)+n\text{-}TiO_2\rightarrow CuFe_2O_4+TiO_2\,(e^-) \quad (6)$$

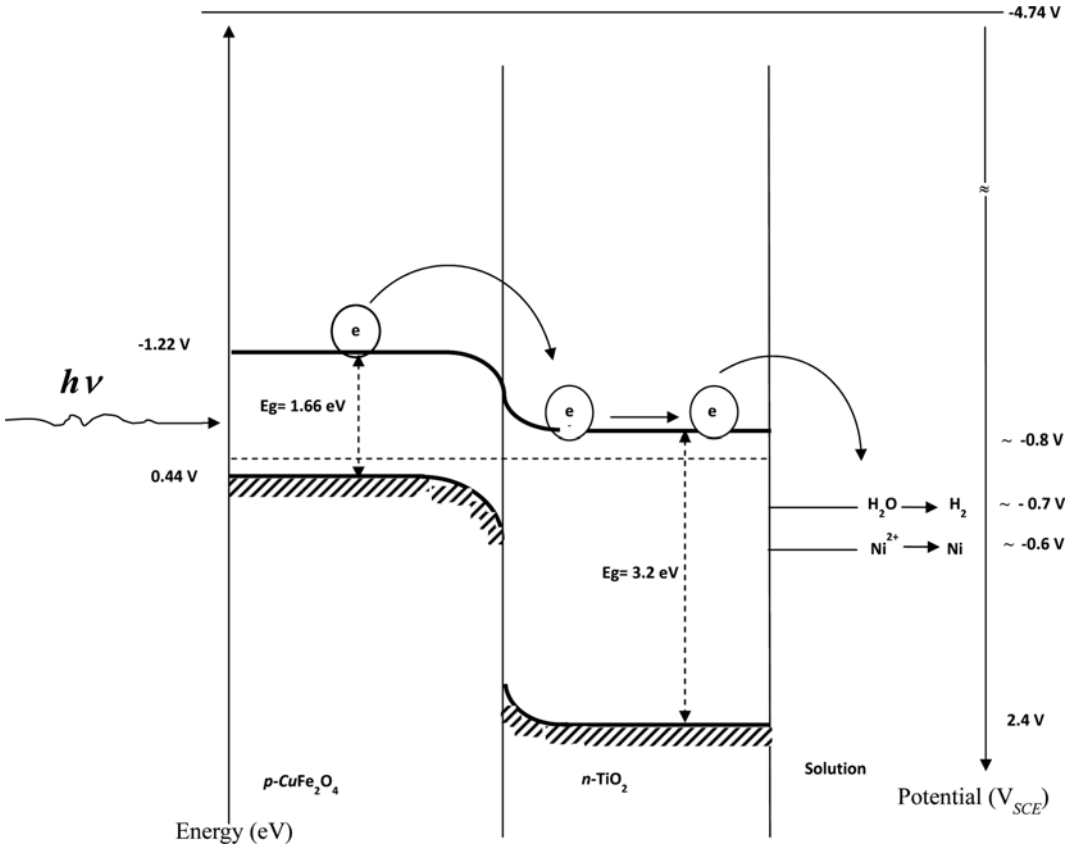

Fig. 5. The energy diagram of the hetero-junction p-$CuFe_2O_4$/n-TiO_2/Ni^{2+}, pH~7).

$$TiO_2\ (2\ e^-)+Ni^{2+}\rightarrow Ni^0+TiO_2 \quad (7)$$

VB being the valence band. The characteristics of TiO_2 were taken from ref. [18].

NICKEL REDUCTION

The Langmuir-Hinshelwood (L-H) model is commonly used for the quantitative treatment of the adsorbent/adsorbate at the solid/liquid interface. The kinetics alone does not indicate whether the process takes place on the surface or in solution [19]. Nevertheless, for the standard L-H treatment, one assumes that the reaction mainly occurs on the surface which is largely accepted. Two extreme cases illustrate the reduction on the catalyst surface [20]: nickel and water compete for the photoelectrons on the active catalytic sites. It should be emphasized that the adsorbed nickel on the TiO_2 surface favors the hydrogen evolution owing of its low over-voltage. The L-H model is expressed as:

$$-\frac{dC}{dt}=\frac{k_rKC}{1+KC} \quad (8)$$

By integrating Eq. (8), one obtains:

$$\ln\left(\frac{C_o}{C}\right)+k_rK(C_o-C)=k_rK\times t \quad (9)$$

If the initial Ni^{2+} concentration (C_o) is smaller than (C), Eq. (9) can be simplified:

$$\ln\left(\frac{C_o}{C}\right)=k_rK\times t \quad (10)$$

where $k=k_rK$ is given by:

$$\ln\left(\frac{C_o}{C}\right)=k\times t \quad (11)$$

Obviously, as explained above (Section: Evaluation of solar radiation), Q_n can substitute the time (t) and the proportionality constant is defined as k_{app}:

$$\ln\left(\frac{C_o}{C}\right)=k_{app}Q_n \quad (12)$$

The Ni^{2+} reduction is carried out in six reactors with the hetero-junction $CuFe_2O_4/TiO_2$ at different concentrations (10-125 ppm) and the curves are reported in Fig. 6(a); the results show the logarithmic slope instead of k_{app} (Fig. 6(b)). Fig. 6(a) represents the six concentrations as a function of Q_n; magnetic agitation is used for dispersing the samples over the whole reaction space. The best performance occurs for a concentration of 30 ppm with an elimination percentage of 72% after 210 min of solar illumination. Our attempts to improve the photoactivity by using reducing agents were unsuccessful. $S_2O_3^{2-}$ was tested and the photoactivity decreased down to 23%.

To confirm the Ni-deposition, we dissolved the metal nickel in

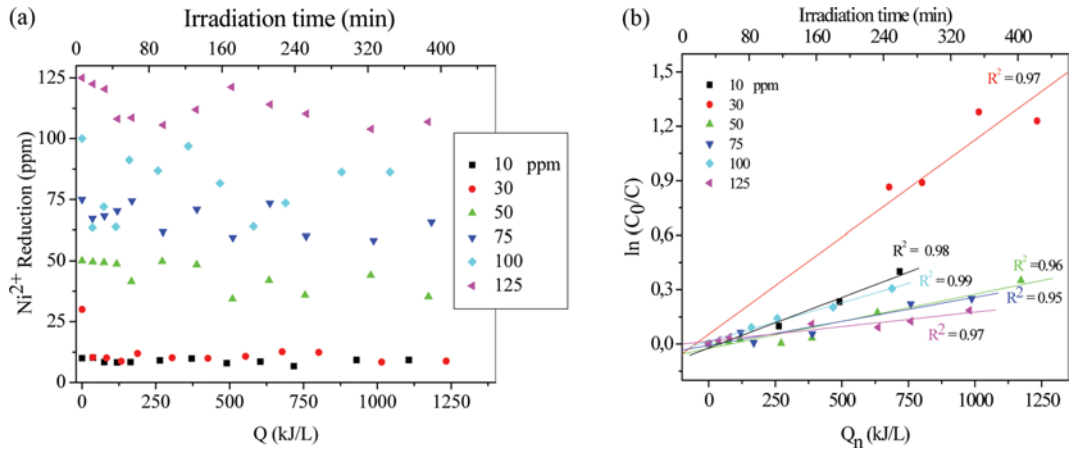

Fig. 6. (a) The variation of the initial concentration (C_o) of Ni^{2+} as a function of Q_n. (b) Ln (C_o/C) as a function of the accumulated solar energy (Q_n).

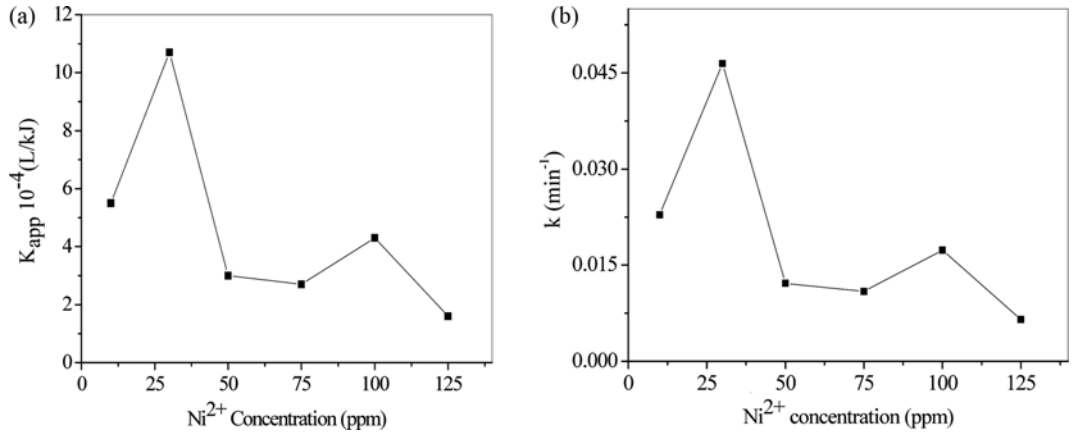

Fig. 7. (a) The rate reaction as a function initial concentration Ni^{2+}. (b) The first order kinetic constant (k).

Table 1. Kinetic parameters of the photo reduction of Ni^{2+} determined from the Langmuir-Hinshelwood model

Ni^{2+} (ppm)	K_{app} (L/kJ)×10^{-4}	$I_{average}$ (W m^{-2})	k (min^{-1})×10^{-2}	R^2	$t_{1/2}$ (min)	$Q_{n\ (total)}$ (kJ/L)
10	5.5	882	2.3	0.98	31	1107
30	10.7	922	4.7	0.97	15	1234
50	3.0	864	1.3	0.96	57	1174
75	2.7	871	1.1	0.95	64	1184
100	4.3	865	1.7	0.99	40	1044
125	1.6	867	0.6	0.97	107	1173

HCl solution and hydrogen was liberated. Therefore, the volume of the evolved hydrogen should be equivalent to the quantity of the deposited nickel. However, the hydrogen volume (1.5 mL) is smaller than that expected (6.3 mL), because of its adsorption on the catalyst powder. Such volume is reliably detected in our experimental device. More interestingly, the solution turns green (characteristic of Ni^{2+}) and the titrated amount of Ni^{2+} (22 ppm) is very close to that determined initially (24 ppm). In addition, the specific surface area decreases from 16.5 to 13.7 m^2 g^{-1} due to the nickel deposition inside the pores.

A similarity of the curves k_{app} and k (=k_rK) is observed (Figs. 7(a) and 7(b)). The best rate constant (k) with an accumulation capacity of 1,234 kJ L^{-1} and a coefficient of 10.7×10^{-4} L kJ^{-1} is obtained for a concentration of 30 ppm (Table 1). The saturation of the catalyst inside the pores needs a higher mass. The experiment performed with 10 ppm is rapid because of the availability of photons, while the catalyst saturation of TiO_2 is due to its small mass. After ~300 min, the elimination of nickel reaches only 30%. For the concentrations 50, 75, 100 and 125 ppm, the same behavior is observed, while the saturation time varies from 180 to 310 min

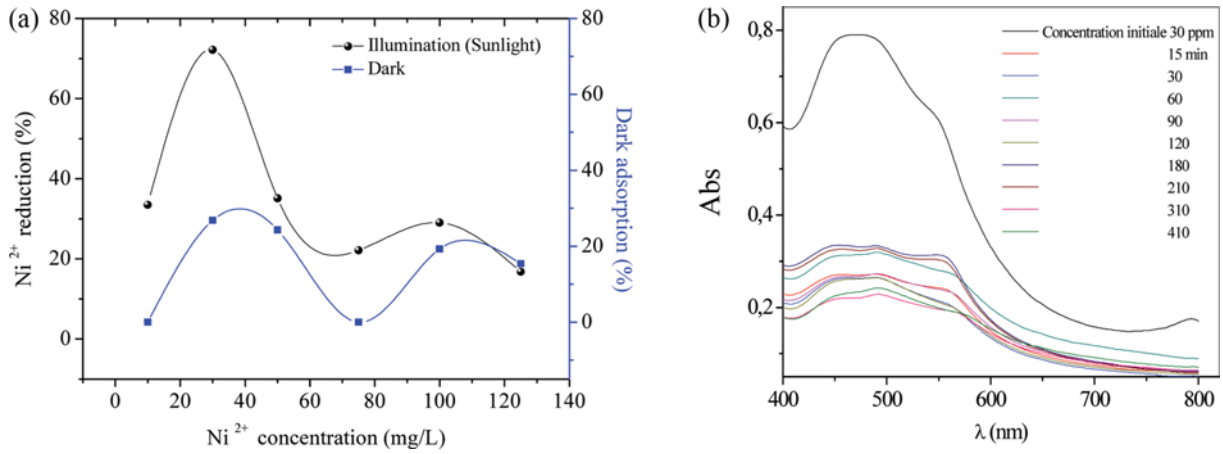

Fig. 8. (a) The variation of the Ni^{2+} reduction rate with the initial concentration. (b) The absorbance as a function of wavelength.

respectively. Concomitantly, the Ni^{2+} reduction increases from 15 to 36% (Fig. 8(a)). Note that the dark adsorption increases similarly with the photocatalysis and a maximum of 26% is reached for Ni^{2+} concentration of 30 ppm (Fig. 8(a)); the tests were repeated three times and the results were reproducible within ±3%. Note also that the XRD patterns of the hetero-junction $CuFe_2O_4/TiO_2$ before and after the photocatalytic tests are very similar, indicating no deterioration of semiconductor materials (SM).

When the concentration C_o is large, the loss of photons is increased; the light absorption becomes difficult in colloid systems and a large reactor is advantageous in such a case. For clarity's sake, we reported in Fig. 8(b) the evolution of UV-Visible spectra over time of Ni^{2+} solution (30 ppm) exposed to sunlight. The evolution of hydrogen onto Ni clusters also accounts for the regression in the photoactivity because of the low over-voltage on nickel [21]. The study in tiny batch gave rise to encouraging results, and the photocatalytic tests will be extended to fluidized bed for the treatment of industrial effluents.

CONCLUSION

The photocatalytic reduction of nickel was carried out in aqueous medium under solar irradiation on the hetero-system $CuFe_2O_4/TiO_2$. The spinel was prepared from nitrates precursors, and the optical gap, determined from the diffuse reflectance, is well suited to the solar spectrum. The photoelectrochemical characterization permitted to draw the energy diagram of $CuFe_2O_4/TiO_2/Ni^{2+}$ solution, a preamble of the photocatalysis. The catalyst concentration was optimized and the best Ni^{2+} concentration led to the conclusion that the light extinction in colloidal suspensions is a determining parameter for the photoreactor design. The best reduction (72%) was with a half-time of 15 min under an average irradiation of 922 W m^{-2}.

ACKNOWLEDGEMENTS

The authors thank R. Ihaddaden, H. Bouchaba, B. Bellal and S. Tebani for their technical assistance. This work was supported financially by the Faculty of Chemistry and Chemical Engineering (Algiers).

SUPPORTING INFORMATION

Additional information as noted in the text. This information is available via the Internet at http://www.springer.com/chemistry/journal/11814.

REFERENCES

1. G. Kim, E. T. Igunnuand and G. Z. Chen, *Chem. Eng. J.*, **244**, 411 (2014).
2. K. Kabra, R. Chaudhary and R. L. Sawhney, *J. Hazard. Mater.*, **155**, 424 (2008).
3. D. J. Sivulka, B. R. Conard, G. W. Hall and J. H. Vincent, *Regulatory Toxicol. Pharmacol.*, **48**, 19 (2007).
4. R. Khlifi, P. Olmedo, F. Gil, B, Hammami, A. Chakroun, A. Rebai and A. Hamza-Chaffai, *Sci. Total Environ.*, **452**, 58 (2013).
5. T. Menné, *Sci. Total Environ.*, **148**, 275 (1994).
6. H. Mekatel, S. Amokrane, B. Bellal, M. Trari and D. Nibou, *Chem. Eng. J.*, **200**, 611 (2012).
7. M. R. Yaiche, A. Bouhanik, S. M. A. Bekkouche, A. Malek and T. Benouaz, *Energy Convers. Manage.*, **82**, 114 (2014).
8. S.-L. Chen, A.-J. Wang, C. Dai, J. B. Benziger and X.-C. Liu, *Chem. Eng. J.*, **249**, 48 (2014).
9. Z. Rui, S. Wu, C. Peng and H. Ji, *Chem. Eng. J.*, **243**, 254 (2014).
10. I. Perraud, R. M. Ayral, C. Cammarano, F. Rouessac, V. Hulea and A. Ayral, *Chem. Eng. J.*, **241**, 360 (2014).
11. A. Moezzi, A. M. McDonagh and M. B. Cortie, *Chem. Eng. J.*, **185**, 1 (2012).
12. J. Feng, L. Su, Y. Ma, C. Ren, Q. Guo and X. Chen, *Chem. Eng. J.*, **221**,16 (2013).
13. Y.-J. Tu, C.-F. You, C.-K. Chang, T.-S. Chan and S.-H. Li, *Chem. Eng. J.*, **244**, 343 (2014).
14. Z. Wang, Q. Li, L. Wang and W. Shangguan, *Appl. Clay Sci.*, **55**, 125 (2012).
15. S. Saadi, A. Bouguelia and M. Trari, *Renew. Energy*, **31**, 2245 (2006).
16. S. Malato, J. Blanco, A. Vidal and C. Richter, *Appl. Catal. B: Envi-*

ron., **37**, 1 (2002).
17. P. Melnikov, V. A. Nascimento, I. V. Arkhangelsky, L. Z. Zanoni-Consolo and L. C. S. de Oliveira, *J. Therm. Anal. Calorim.*, **115**, 145 (2014).
18. R. Brahimi, Y. Bessekhouad, A. Bouguelia and M. Trari, *J. Photochem. Photobiol. A: Chem.*, **194**, 173 (2008).
19. P. Fernández-Ibáñez, S. Malato and F. J. de las Nieves, *Catal. Today*, **54**, 195 (1999).
20. N. Serpone, P. Maruthamuthu, P. Pichat, E. Pelizzetti and H. Hidaka, *J. Photochem. Photobiol. A: Chem.*, **85**, 247 (1995).
21. A. YahiaCherif, O. Arous, M. Amara, S. Omeiri, H. Kerdjoudjf and M. Trari, *J. Hazard. Mater.*, **227**, 386 (2012).

Supporting Information

Ni^{2+} reduction under solar irradiation over $CuFe_2O_4/TiO_2$ catalysts

Maamar Fedailaine, Sabrina Berkani, and Mohamed Trari†

Laboratory of Storage and Valorization Renewable Energies (USTHB), BP 32 El-Alia 16111 Algiers, Algeria
(*Received 31 December 2014 • accepted 22 February 2016*)

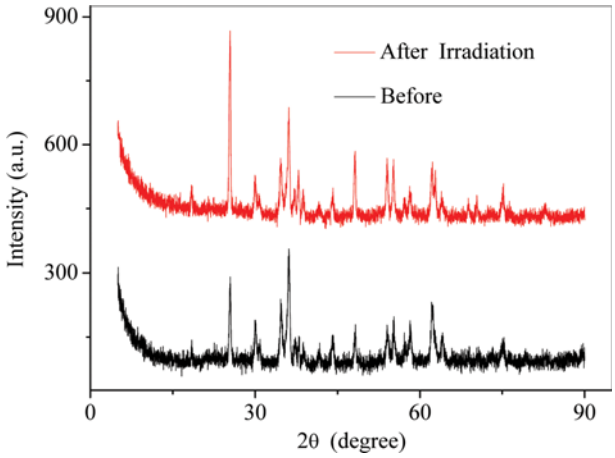

Fig. S1. The XRD patterns of the hetero-system $CuFe_2O_4/TiO_2$ before and after the photocatalytic test.